Joint UAV Trajectory and Transmission Scheduling Optimization for User Localization

Nguyen Van Cuong[†], Chau Thi Ngoc Loan[‡], Y.-W. Peter Hong[*], and Jang-Ping Sheu[*†],
[†]Department of Computer Science, National Tsing Hua University, Taiwan
[*]Institute of Communications Engineering, National Tsing Hua University, Taiwan
[‡] Department of Electrical Engineering, Yuan Ze University, Taiwan
Emails: cuongnv@gapp.nthu.edu.tw, loanchau.rosie@gmail.com, {ywhong@ee, sheujp@cs}.nthu.edu.tw

GLOBECOM 2025 - 2025 IEEE Global Communications Conference | 979-8-3315-7781-0/25/$31.00 ©2025 IEEE | DOI: 10.1109/GLOBECOM59602.2025.11431940

***Abstract*—This work examines the use of unmanned aerial vehicles (UAVs) as mobile anchors to determine the locations of ground users based on the received signal strength (RSS). This is motivated by the significance of user location information in search and rescue operations, post-disaster recovery, and wireless communication systems. By utilizing the Cramér-Rao lower bound (CRLB) as a measure of localization accuracy, we jointly optimize the UAV's flight trajectory and the users' transmission scheduling for localization. We propose an iterative solution in which the transmission scheduling and trajectory design subproblems are solved in turn until convergence. We utilize a successive convex approximation (SCA) approach to address the non-convexity of the transmission scheduling subproblem and adopt a gradient descent method to solve the UAV trajectory optimization subproblem. Extensive simulation results verify that our proposed solution outperforms various baselines.**

***Index Terms*—UAV trajectory optimization, transmission scheduling, user localization.**

I. Introduction

Radio signal localization is critical in many applications, such as search and rescue missions and mobile communication systems. In the context of rescue missions, it enables the detection of victims trapped under collapsed buildings during earthquakes or the tracking of individuals in remote or hostile areas. In these cases, localization by the Global Positioning System (GPS) may not always be available due to the lack of GPS modules on user devices or due to signal blockage in disaster sites [1]. In mobile communication systems, accurate user location information is essential for optimizing network performance. For instance, cellular network operators leverage geographic user distribution data to enhance network planning and resource allocation [2]. Similarly, in the Internet of Things (IoT), sensor nodes are typically low-cost and battery-constrained, and thus often lack GPS modules, necessitating the adoption of alternative localization methods [3].

Unmanned aerial vehicles (UAVs) offer notable advantages, making them increasingly popular in various applications. In wireless signal-based localization, UAVs equipped with GPS modules can be deployed as aerial anchor nodes to receive positioning signals from ground users. Due to their high mobility, UAVs can collect signal observations at different locations, thereby reducing localization error and the number of waypoints needed in localization [4]. Optimizing the UAV trajectory and the users' transmission scheduling is essential to achieve good performance in UAV-assisted user localization. This is because the localization accuracy is highly affected by the location where signals are observed [5]. A poor geometry deployment of anchor nodes, e.g., collinear points, often results in a high error in location estimation. Furthermore, because of power-saving transmission modes and possibly shared frequency channels, users' devices cannot continuously send signals during the mission time. In this case, the users' transmissions must be optimally scheduled to improve the effectiveness of the signal measurements at the UAV.

UAV trajectory optimization for user localization has been investigated in previous works in the literature [4], [6]–[9]. For example, the works in [4] and [6] optimized the trajectory of a single UAV that served as an aerial anchor node to localize terrestrial users based on the received signal strength (RSS). Also measuring RSSs emitted from ground users, [7] used a UAV equipped with an array antenna and followed a predefined trajectory. A score map was constructed from the measured power, which was then used to estimate the users' locations. [8] examined the placement of moving aerial anchors to localize mobile users while considering their energy consumption issues. In [9], a UAV-aided positioning system was proposed to determine the positions of ground devices using a hybrid method of time of arrival (ToA) and angle of arrival (AoA) techniques. An algorithm was proposed to deploy the UAVs iteratively to optimize the Cramér-Rao lower bound (CRLB) criterion of the positioning process.

Several recent works have jointly optimized UAV trajectory, resource allocation, and transmission scheduling, particularly in integrated localization and communications (ILAC) systems [10]–[12]. For example, in [10], a UAV was incorporated with ground base stations to serve data collection and localization. UAV trajectory and transmission schedules were determined to minimize sensors' energy consumption. [11] also investigated an ILAC network assisted by UAVs. They jointly solved the UAV placement, bandwidth, and power allocation problems to maximize the communication rate under localization error constraints. [12] used multiple UAVs to collect data and locate

This work was supported in part by the National Science and Technology Council, Taiwan, under grants 112-2811-E-007-036-MY3 and 114-2221-E-007-007.

sensor nodes. By jointly optimizing the UAV trajectories and sensor transmission schedule, their goal was to minimize the localization error under the constraint of the amount of user data uploaded. Most of the above works placed the UAVs in fixed locations or restricted their movement on predefined paths, thus not fully utilizing their mobility. These works also do not fully examine the joint impact of UAV trajectory and transmission scheduling on the localization accuracy.

This work examines the use of a UAV as a moving aerial anchor to localize ground users based on the wireless signals emitted from the users. The RSS-based localization method is employed due to its simplicity and the availability of RSS information on most wireless devices. Our main objective is to minimize localization errors by jointly designing the UAV trajectory and transmission scheduling. The main contributions can be summarized as follows:

- We utilize the UAV's mobility to enhance the quality and diversity of radio signals received from ground users for localization purposes.
- The CRLB is used as a measure of localization accuracy, and a joint trajectory and transmission scheduling design problem is formulated based on the minimization of the approximate CRLB. This results in a mixed-integer nonlinear programming (MINLP) problem that is generally difficult to solve.
- We propose an iterative solution where the transmission scheduling and flight trajectory are optimized in turn until convergence. We adopt a successive convex approximation (SCA) approach to cope with the nonconvexity of the transmission scheduling subproblem and a gradient descent method to solve the trajectory design subproblem.
- Simulation results are provided to demonstrate the effectiveness of the proposed algorithm compared to several existing methods in the literature.

The rest of this paper is organized as follows. In Section II, we describe the system model and formulate the problem. The proposed solution is presented in Section III. Section IV provides simulation results to demonstrate the effectiveness of the proposed algorithm. Finally, we conclude in Section V.

II. System Model and Problem Formulation

We consider a system in which a UAV is deployed as a mobile anchor to estimate the location of M ground users. The localization by the UAV is performed based on the RSS of signals received from the users over N equal-length time slots. The users are deployed over an $L\times W$ m^2 region, as illustrated in Fig. 1, with positions $\{\mathbf{u}_m \triangleq (x_m, y_m, 0)\}_{m=1}^{M}$ that are to be estimated by the UAV. Before the mission, coarse estimates of user positions, denoted by $\hat{\mathbf{u}}_m$, are assumed to be available. This can be obtained, for example, by users transmitting their signals over different time slots, with a transmission schedule that is broadcast to them by the UAV at the beginning of each signal collection round. The position of the UAV in time slot n is indicated by $\mathbf{q}[n] \triangleq (x[n], y[n], h)$, where h is the fixed altitude, e.g., to obey government regulations. A binary

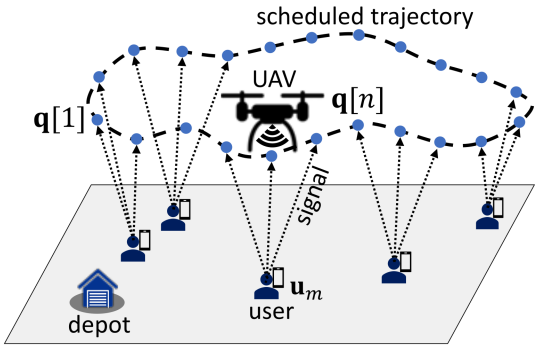

Fig. 1: System model

scheduling variable $a_m[n]$ is defined such that $a_m[n] = 1$ if user m is scheduled to transmit in the time slot n and $a_m[n] = 0$, otherwise.

A. Channel Model

In this work, the localization at the UAV is performed based on the RSS of the signals received from the users. The user-to-UAV channel follows the log-normal shadowing model, which is widely used in the literature [5], [13], [14]. The UAV position is considered fixed during the duration of a time slot, resulting in a stable channel in each time slot. The RSS (in dBm) of the signal sent by user m to the UAV in time slot n is modeled by

$$P_m[n] = P_0 - 10\alpha \log_{10} \frac{\|\mathbf{q}[n] - \mathbf{u}_m\|}{d_0} + \zeta, \qquad (1)$$

where P_0 represents the reference power (in dBm) measured at a distance d_0, α is the path loss exponent, and $\zeta \sim \mathcal{N}(0, \sigma^2)$ represents the random shadowing noise.

B. Cramér-Rao Lower Bound

In this work, we utilize the Cramér-Rao lower bound (CRLB) [15] as a measure of localization accuracy based on the RSSs collected from the users. Note that the locations of the UAV during the collection of users' signals can have a significant impact on localization accuracy. Specifically, let $\mathcal{N}_m \triangleq \{n : a_m[n] = 1\}$ be the set of time slots for which user m is scheduled to transmit, and let $\mathcal{P}_m \triangleq \{P_m[n], \forall n \in \mathcal{N}_m\}$ be the set of RSSs collected from user m. Note that $|\mathcal{N}_m| = \sum_{n=1}^{N} a_m[n]$. The log-likelihood function of observations associated with user m can be expressed as

$$\begin{aligned}
&\ln p(\mathcal{P}_m; \mathbf{u}_m) \\
&= -\frac{1}{2\sigma^2} \sum_{n\in\mathcal{N}_m} \left(P_0 - 10\alpha \log_{10} \frac{\|\mathbf{q}[n] - \mathbf{u}_m\|}{d_0} - P_m[n]\right)^2 \\
&\quad - \frac{|\mathcal{N}_m|}{2} \ln(2\pi\sigma^2) \\
&= -\frac{1}{2\sigma^2} \sum_{n=1}^{N} a_m[n] \left(P_0 - 10\alpha \log_{10} \frac{\|\mathbf{q}[n] - \mathbf{u}_m\|}{d_0} - P_m[n]\right)^2 \\
&\quad - \frac{\sum_{n=1}^{N} a_m[n]}{2} \ln(2\pi\sigma^2). \qquad (2)
\end{aligned}$$

In this case, the Fisher Information Matrix (FIM) [15] can be computed as

$$\mathbf{I}(\mathbf{u}_m) = \begin{bmatrix} -\mathbb{E}\big[\frac{\partial^2 \ln p(\mathcal{P}_m;\mathbf{u}_m)}{\partial x_m \partial x_m}\big] & -\mathbb{E}\big[\frac{\partial^2 \ln p(\mathcal{P}_m;\mathbf{u}_m)}{\partial x_m \partial y_m}\big] \\ -\mathbb{E}\big[\frac{\partial^2 \ln p(\mathcal{P}_m;\mathbf{u}_m)}{\partial x_m \partial y_m}\big] & -\mathbb{E}\big[\frac{\partial^2 \ln p(\mathcal{P}_m;\mathbf{u}_m)}{\partial y_m \partial y_m}\big] \end{bmatrix}, \quad (3)$$

where $-\mathbb{E}\left[\frac{\partial^2 \ln p(\mathcal{P}_m;\mathbf{u}_m)}{\partial x_m \partial x_m}\right] = \omega \sum_{n=1}^{N} a_m[n] \frac{(x[n]-x_m)^2}{\|\mathbf{q}[n]-\mathbf{u}_m\|^4}$, $-\mathbb{E}\left[\frac{\partial^2 \ln p(\mathcal{P}_m;\mathbf{u}_m)}{\partial y_m \partial y_m}\right] = \omega \sum_{n=1}^{N} a_m[n] \frac{(y[n]-y_m)^2}{\|\mathbf{q}[n]-\mathbf{u}_m\|^4}$, $-\mathbb{E}\left[\frac{\partial^2 \ln p(\mathcal{P}_m;\mathbf{u}_m)}{\partial x_m \partial y_m}\right] = \omega \sum_{n=1}^{N} a_m[n] \frac{(x[n]-x_m)}{\|\mathbf{q}[n]-\mathbf{u}_m\|^2} \frac{(y[n]-y_m)}{\|\mathbf{q}[n]-\mathbf{u}_m\|^2}$, and $\omega \triangleq \frac{10\alpha}{\sigma \ln(10)}$. Note that $\mathbb{E}[P_m[n]] = P_0 - 10\alpha \log_{10} \frac{\|\mathbf{q}[n]-\mathbf{u}_m\|}{d_0}$ since the random shadowing noise in (1) has zero mean. Therefore, the CRLB of the estimate of user m's location can be written as

$$\begin{aligned} &\mathrm{CRLB}(\mathbf{u}_m) \\ &= \mathrm{tr}\big(\mathbf{I}^{-1}(\mathbf{u}_m)\big) \\ &= \frac{1}{\omega^2}\Bigg(\sum_{n=1}^{N} \frac{a_m[n]}{\|\mathbf{q}[n]-\mathbf{u}_m\|^2}\Bigg) \Bigg/ \\ &\quad \Bigg[\sum_{n=1}^{N} a_m[n] \frac{(x[n]-x_m)^2}{\|\mathbf{q}[n]-\mathbf{u}_m\|^4} \sum_{n=1}^{N} a_m[n] \frac{(y[n]-y_m)^2}{\|\mathbf{q}[n]-\mathbf{u}_m\|^4} \\ &\quad - \Big(\sum_{n=1}^{N} a_m[n] \frac{(x[n]-x_m)}{\|\mathbf{q}[n]-\mathbf{u}_m\|^2} \frac{(y[n]-y_m)}{\|\mathbf{q}[n]-\mathbf{u}_m\|^2}\Big)^2\Bigg]. \end{aligned} \quad (4)$$

C. Problem Formulation

In this work, we aim to jointly optimize the UAV trajectory and transmission scheduling by minimizing the average approximate CRLB of the location estimates of all users, i.e.,

$$\min_{\mathbf{q}[n], a_m[n], \forall m,n} \ \frac{1}{M} \sum_{m=1}^{M} \mathrm{CRLB}(\hat{\mathbf{u}}_m) \quad (5a)$$

$$\text{subject to} \quad a_m[n] \in \{0,1\}, \sum_{m=1}^{M} a_m[n] = 1, \ \forall m, n, \quad (5b)$$

$$\|\mathbf{q}[n] - \mathbf{q}[n+1]\| \le d_{\max}, \forall n \le N-1, \quad (5c)$$

$$\mathbf{q}[1] = \mathbf{p}, \mathbf{q}[N] = \mathbf{p}\ , \quad (5d)$$

where (5b) guarantees that each slot is assigned to only one user, (5c) restricts the UAV movement in consecutive time slots to a given distance $d_{\max}$, and (5d) requires the UAV to depart and return to a given depot $\mathbf{p}$. Note that the approximate CRLBs are CRLBs evaluated at the known coarse locations of the users, i.e., $\hat{\mathbf{u}}_m$, for all m, since the true locations are not available. The problem in (5) is a mixed-integer nonlinear programming (MINLP) problem that is challenging to solve. In the following, we propose an iterative algorithm to obtain an efficient solution for the above problem, utilizing SCA and gradient descent methods to address the non-convexity.

III. The Proposed CRLB-Minimizing UAV Trajectory and User Scheduling Algorithm

In this section, we present an approximate CRLB-minimizing (approximate CRLB-Min) UAV trajectory and user scheduling algorithm to obtain an efficient solution for the problem in (5). The proposed algorithm decomposes the main problem into two subproblems, including the transmission scheduling and UAV trajectory optimization subproblems as follows.

A. Subproblem I: User Scheduling Optimization

Given the trajectory $\mathbf{q}^{(i)}[n]$ after iteration i, the transmission scheduling subproblem in iteration $i+1$ is

$$\min_{a_m[n], \forall m,n} \ \frac{1}{M} \sum_{m=1}^{M} \mathrm{CRLB}(\hat{\mathbf{u}}_m) \quad (6a)$$

$$\text{subject to} \quad a_m[n] \in \{0,1\}, \sum_{m=1}^{M} a_m[n] = 1, \forall m, n, \quad (6b)$$

which is also an MINLP problem. We begin by relaxing the binary variables $a_m[n]$ and introducing a penalty term to the objective, thereby promoting a binary solution. Next, we deal with the approximate CRLB term in the objective, which is a nonconvex function. An auxiliary variable c_m is introduced satisfying $\mathrm{CRLB}(\hat{\mathbf{u}}_m) \le c_m$. To obtain a more tractable form of this constraint, we further introduce auxiliary variables z_m, s_m, and θ_M. The problem is reformulated to

$$\min_{\substack{a_m[n], c_m, z_m, \\ s_m, \theta_m, \forall m,n}} \ \frac{1}{M}\sum_{m=1}^{M} c_m + \lambda \sum_{n=1}^{N}\sum_{m=1}^{M} (a_m[n] - a_m[n]^2) \quad (7a)$$

subject to

$$0 \le a_m[n] \le 1, \ \sum_{m=1}^{M} a_m[n] = 1, \ \forall m, n, \quad (7b)$$

$$\sum_{n=1}^{N} \frac{a_m[n]}{\|\mathbf{q}^{(i)}[n] - \hat{\mathbf{u}}_m\|^2} \le z_m - s_m, \ \forall m, \quad (7c)$$

$$c_m \omega^2 \Bigg(\sum_{n=1}^{N} \frac{a_m[n](x^{(i)}[n] - \hat{x}_m)^2}{\|\mathbf{q}^{(i)}[n] - \hat{\mathbf{u}}_m\|^4}\Bigg) \times \Bigg(\sum_{n=1}^{N} \frac{a_m[n](y^{(i)}[n] - \hat{y}_m)^2}{\|\mathbf{q}^{(i)}[n] - \hat{\mathbf{u}}_m\|^4}\Bigg) \ge z_m, \ \forall m, \quad (7d)$$

$$c_m \omega^2 \theta_m \le s_m, \ \forall m, \quad (7e)$$

$$\Bigg(\sum_{n=1}^{N} a_m[n] \frac{x^{(i)}[n] - \hat{x}_m}{\|\mathbf{q}^{(i)}[n] - \hat{\mathbf{u}}_m\|^2} \frac{y^{(i)}[n] - \hat{y}_m}{\|\mathbf{q}^{(i)}[n] - \hat{\mathbf{u}}_m\|^2}\Bigg)^2 \le \theta_m \ \forall m. \quad (7f)$$

The above problem remains nonconvex due to the nonconvexity of the objective and constraints (7d) and (7e). First, the penalty term $\lambda \sum_{m=1}^{M}\sum_{n=1}^{N}(a_m[n] - a_m^2[n])$ is concave w.r.t. $a_m[n]$. Thus, it can be upper-bounded by the first-order Taylor expansion at the point $a_m^{(i)}[n]$. That is

$$\begin{aligned} &\lambda \sum_{m=1}^{M}\sum_{n=1}^{N}(a_m[n] - a_m^2[n]) \\ &\le \lambda \sum_{m=1}^{M}\sum_{n=1}^{N}(a_m^{(i)}[n])^2 + a_m[n](1 - 2a_m^{(i)}[n]). \end{aligned} \quad (8)$$

Next, by taking the logarithm on both sides of (7d) and then replacing the right-hand side (RHS) with the first-order Taylor expansion, we derive the following convex constraint

$$\ln(c_m\omega^2)+\ln\left(\sum_{n=1}^{N}\frac{a_m[n](x^{(i)}[n]-\hat{x}_m)^2}{\|\mathbf{q}^{(i)}[n]-\hat{\mathbf{u}}_m\|^4}\right)+\ln\left(\sum_{n=1}^{N}\frac{a_m[n](y^{(i)}[n]-\hat{y}_m)^2}{\|\mathbf{q}^{(i)}[n]-\hat{\mathbf{u}}_m\|^4}\right)\geq \ln z_m^{(i)}+\frac{z_m-z_m^{(i)}}{z_m^{(i)}}. \quad (9)$$

Similarly, the constraint (7e) can be approximated to

$$\ln c_m^{(i)}+\frac{c_m-c_m^{(i)}}{c_m^{(i)}}+\ln\omega^2+\ln\theta_m^{(i)}+\frac{\theta_m-\theta_m^{(i)}}{\theta_m^{(i)}}\leq \ln s_m. \quad (10)$$

To this end, by replacing the penalty term in objective (7a) with the RHS of (8), and replacing (7d) and (7e) with their convex approximations in (9) and (10), respectively, we obtain a convex optimization problem as

$$\min_{\substack{a_m[n],c_m,z_m,\\ s_m,\theta_m,\forall m,n}} \frac{1}{M}\sum_{m=1}^{M}c_m+\lambda\sum_{m=1}^{M}\sum_{n=1}^{N}\Big((a_m^{(i)}[n])^2+a_m[n](1-2a_m^{(i)}[n])\Big) \quad (11a)$$

$$\text{subject to} \quad (7b),\ (7c),\ (7f),\ (9),\ (10). \quad (11b)$$

The problem (11) is a convex optimization problem that can be solved efficiently using optimization tools, e.g., CVX.

B. Subproblem II: UAV Trajectory Optimization

Given $a_m^{(i+1)}[n]$ from solving Subproblem I, the UAV trajectory optimization subproblem is expressed as

$$\min_{\mathbf{q}[n],\forall m,n} \frac{1}{M}\sum_{m=1}^{M}\text{CRLB}(\hat{\mathbf{u}}_m) \quad (12a)$$

$$\text{subject to} \quad (5c),\ (5d). \quad (12b)$$

The objective of problem (12) is highly nonconvex w.r.t.$\mathbf{q}[n]$. We address this issue using a gradient descent method as follows. We first incorporate the constraint (5c) as a penalty term in the objective and rewrite the problem as

$$\min_{\substack{\mathbf{q}[n],\\ 2\leq n\leq N-1}} \frac{1}{M}\sum_{m=1}^{M}\text{CRLB}(\hat{\mathbf{u}}_m)+\mu\sum_{n=1}^{N-1}\max\left(\|\mathbf{q}[n]-\mathbf{q}[n+1]\|-d_{\max},0\right)^2, \quad (13)$$

where μ represents the penalty parameter. Note that the constraint (5d) is omitted here as it can be satisfied during trajectory initialization and then is not updated further. The unconstrained optimization problem in (13) can be solved using the gradient descent method. For the sake of presentation, we rewrite the approximate CRLB in (13) as $\text{CRLB}(\hat{\mathbf{u}}_m)=\frac{1}{\omega^2}\frac{A_m}{(E_mF_m-B_m)}$, where $A_m\triangleq\sum_{n=1}^{N}\frac{a_m^{(i+1)}[n]}{\|\mathbf{q}[n]-\hat{\mathbf{u}}_m\|^2}$, $B_m\triangleq\left(\sum_{n=1}^{N}\frac{a_m^{(i+1)}[n](x[n]-\hat{x}_m)(y[n]-\hat{y}_m)}{\|\mathbf{q}[n]-\hat{\mathbf{u}}_m\|^4}\right)^2$, $E_m\triangleq\sum_{n=1}^{N}\frac{a_m^{(i+1)}[n](x[n]-\hat{x}_m)^2}{\|\mathbf{q}[n]-\hat{\mathbf{u}}_m\|^4}$, and $F_m\triangleq\sum_{n=1}^{N}\frac{a_m^{(i+1)}[n](y[n]-\hat{y}_m)^2}{\|\mathbf{q}[n]-\hat{\mathbf{u}}_m\|^4}$.

The gradient of $\text{CRLB}(\hat{\mathbf{u}}_m)$ w.r.t. coordinate $x[n]$ can be expressed as

$$\frac{\partial\text{CRLB}(\hat{\mathbf{u}}_m)}{\partial x[n]}=\frac{1}{\omega^2}\left[\frac{\partial A_m}{\partial x[n]}(E_mF_m-B_m)-A_m\Big(\frac{\partial(E_mF_m)}{\partial x[n])}-\frac{\partial B_m}{\partial x[n]}\Big)\right]\Big/\big(E_mF_m-B_m\big)^2, \quad (14)$$

where $\frac{\partial A_m}{\partial x[n]}=-\frac{2a_m^{(i+1)}[n](x[n]-\hat{x}_m)}{\|\mathbf{q}[n]-\hat{\mathbf{u}}_m\|^4}$, $\frac{\partial(E_mF_m)}{\partial x[n]}=a_m^{(i+1)}[n]\frac{2(x[n]-\hat{x}_m)\|\mathbf{q}[n]-\hat{\mathbf{u}}_m\|^2-4(x[n]-\hat{x}_m)^3}{\|\mathbf{q}[n]-\hat{\mathbf{u}}_m\|^6}F_m-4E_ma_m^{(i+1)}[n]\frac{(y[n]-\hat{y}_m)^2(x[n]-\hat{x}_m)}{\|\mathbf{q}[n]-\hat{\mathbf{u}}_m\|^6}$, and $\frac{\partial B_m}{\partial x[n]}=2B_ma_m^{(i+1)}[n]\frac{(y[n]-\hat{y}_m)\left[\|\mathbf{q}[n]-\hat{\mathbf{u}}_m\|^2-4(x[n]-\hat{x}_m)^2\right]}{\|\mathbf{q}[n]-\hat{\mathbf{u}}_m\|^6}$.

Furthermore, let $f_m[n][n']\triangleq\max(\|\mathbf{q}[n]-\mathbf{q}[n']\|-d_{\max},0)^2$. Its gradient w.r.t. $x[n]$ can be computed as

$$\frac{\partial f_m[n][n']}{\partial x[n]}=\begin{cases}\frac{2f_m[n][n'](x[n]-x[n'])}{\|\mathbf{q}[n]-\mathbf{q}[n']\|}, & \text{if } \|\mathbf{q}[n]-\mathbf{q}[n']\|-d_{\max}\geq 0;\\ 0, & \text{otherwise.}\end{cases} \quad (15)$$

Given $\mathbf{q}^{(j)}[n]=(x^{(j)}[n],y^{(j)}[n])$ as the trajectory in iteration j of the gradient descent process. By (14) and (15), the x coordinate of the trajectory in iteration $j+1$ is updated by

$$x^{(j+1)}[n]=x^{(j)}[n]-\gamma\left[\frac{1}{M}\sum_{m=1}^{M}\frac{\partial\text{CRLB}(\hat{\mathbf{u}}_m)}{\partial x^{(j)}[n]}+\mu\Big(\frac{\partial(f_m[n][n+1]^2)}{\partial x^{(j)}[n]}+\frac{\partial(f_m[n][n-1]^2)}{\partial x^{(j)}[n]}\Big)\right], \quad (16)$$

for all $2\leq n\leq N-1$, where γ accounts for the learning rate. It is worth noting that (16) involves penalty terms to both the preceding and next time slots since $\mathbf{q}[n]$ and $\mathbf{q}[n+1]$ are coupled in (13). The y coordinate can be updated similarly. The update process is repeated until convergence or reaching a given maximum number of iterations.

The proposed iterative algorithm is summarized in Algorithm 1, where two subproblems are solved in turn until convergence, i.e., the objective is no longer improved after scheduling variables $a_m[n]$ return binary. Note that the penalty parameter λ is initially set to be small to give flexibility to the optimization but then is gradually increased to promote binary solutions of $a_m[n]$. Solving the convex optimization problem of Subproblem I in (11) with the interior point method requires a computational complexity of $\mathcal{O}\big((NM+4M)^3\log\frac{1}{\tau}\big)$, where $NM+4M$ is the number of variables and τ accounts for the desired accuracy [16]. The complexity of Subproblem II mainly depends on computing the gradient of approximate CRLB in (14), where each user requires a complexity of $\mathcal{O}(N)$. Since there are M users and $N-2$ time slots need to be computed, and the maximum number of iterations is set to J, the complexity in the worst case is roughly $\mathcal{O}(JMN(N-2))$. Thus, the overall complexity of Algorithm 1 is $\mathcal{O}(I((NM+4M)^3\log\frac{1}{\tau}+JMN(N-2)))$, where I is the number of outer iterations.

Algorithm 1: Approximate CRLB-Min UAV Trajectory and User Scheduling Algorithm

Initialize trajectory $\mathbf{q}^{(0)}[n]$, user scheduling $a_m^{(0)}[n]$, and penalty parameters λ ; set $\text{Obj}^{[0]} = 0$, $i = 0$;
repeat
  Given $\mathbf{q}^{(i)}[n], a_m^{(i)}[n], \theta_m^{(i)}, c_m^{(i)}, z_m^{(i)}$, solve subproblem I in (11) to obtain $a_m^{(i+1)}[n]$, $\theta_m^{(i+1)}$, $c_m^{(i+1)}$, and $z_m^{(i+1)}$, $\forall m, n$;
  Given $\mathbf{q}^{(i)}[n], a_m^{(i+1)}[n]$, solve subproblem II in (16) to obtain $\mathbf{q}^{(i+1)}[n], \forall n$;
  Update $\lambda \leftarrow \rho \times \delta$, where $\rho > 1$, for every δ iterations ;
  Set $i \leftarrow i + 1$;
until $a_m[n] \in \{0, 1\}, \forall m, n$, and $\frac{|\text{Obj}^{[i]} - \text{Obj}^{[i-1]}|}{|\text{Obj}^{[i-1]}|} < \epsilon$;
Return $\mathbf{q}^*[n] = \mathbf{q}^{(i)}[n]$ and $a_m^*[n] = a_m^{(i)}[n]$, $\forall m, n$;

IV. Performance Evaluation

This section provides simulation results to validate the efficiency of the proposed algorithms. Unless mentioned otherwise, we set $M = 10$, $N = 100$, and $\sigma = 2.5$ dB. Users' true positions $\mathbf{u}_m$ are uniformly placed in an area of 500×500 m^2. The coarse positions are assumed to be $\hat{\mathbf{u}}_m \sim \mathcal{N}(\mathbf{u}_m, 30\text{ m})$. The transmission channel is set with $P_0 = -40$ dBm and $\alpha = 2$. Regarding UAV's movement, we set $h = 50$ m, $d_{\max} = 20$ m, and the depot $\mathbf{p}$ is randomly located in the region. Apart from the average true CRLB (i.e., average CRLB evaluated at $\mathbf{u}_m$), we consider the root mean square error (RMSE) metric to demonstrate the effectiveness of approximate CRLB minimization in our work. It is computed by $\text{RMSE} = \sqrt{\frac{\sum_{t=1}^{T}\sum_{m=1}^{M}\|\hat{\mathbf{u}}_m^{(t)} - \mathbf{u}_m\|^2}{T \times M}}$, where $T = 500$ is the number of realizations in the simulation and $\hat{\mathbf{u}}_m^{(t)}$ indicates user m's location estimate in realization t. Here, we apply the extended Kalman filter (EKF) [15] to estimate it based on RSS data the UAV collected, and the mean square error matrix is initialized as $\begin{bmatrix} 2000 & 0 \\ 0 & 2000 \end{bmatrix}$.

Several baselines are implemented, combining the following transmission scheduling and trajectory strategies. Given a trajectory, *Greedy Scheduling (Greedy Sched)* sequentially associates users with the nearest distance-time slots until all time slots are assigned. *Spiral Trajectory (Spiral Traj)* indicates the spiral path with the best objective that is selected from a set of 50 spirals centered in the network area, starting with different radii, i.e., 250 m, 249.5 m, ..., and reducing by 1 m per time slot. They begin at the point closest to the depot and end where the UAV can still return to the depot before slot N. The UAV flies at the maximum speed, and the depot connects to the spiral's start and end via elliptical arcs rather than straight lines. *Particle Swarm Optimization-based Trajectory (PSO Traj)* employs the PSO algorithm to optimize the UAV trajectory as proposed in [12]. It is configured with a cognitive coefficient $= 1.5$, a social coefficient $= 1.5$, and an inertia weight $= 0.7$. *Differential Evolution-based Trajectory (DE Traj)* employs the DE algorithm to optimize the UAV trajectory, as proposed in [10], while setting both the mutation factor and crossover probability parameters to 0.8. Both PSO Traj and DE Traj handle the constraint by the penalty method. They are initialized with the spiral paths above and stop after 200 iterations. The solution of spiral trajectory and greedy scheduling is also the initialization for the proposed scheme.

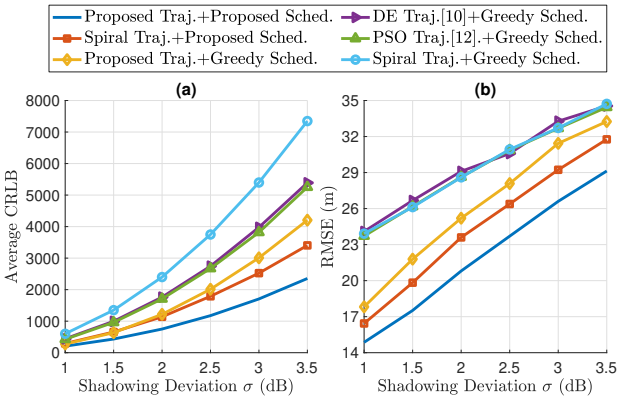

Fig. 2: Average CRLB and RMSE versus shadowing deviation σ

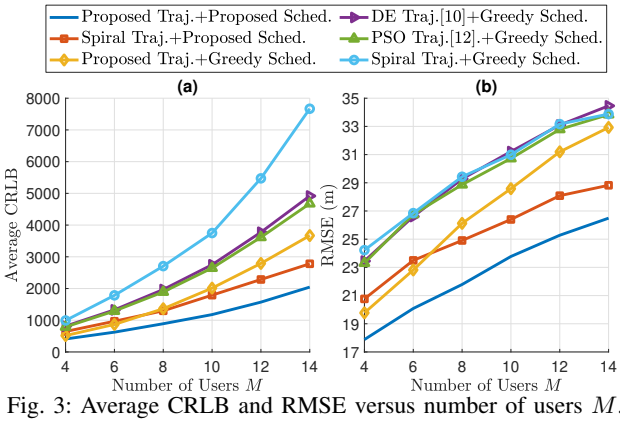

Fig. 3: Average CRLB and RMSE versus number of users M.

Fig. 2(a) shows the average CRLB with different deviations of the shadowing noise. At low noise, the RSS-based ranging is more accurate, leading to a good localization lower bound in all schemes. As noise increases, the accuracy of the RSS-based ranging degrades, raising the CRLB. Our proposed scheme outperforms all baselines since the gradient of the closed-form CRLB expression provides a good direction to obtain a sub-optimal trajectory, and the proposed transmission scheduling can optimally associate time slots and users according to the users' deployment. The PSO-based and DE-based trajectories may highly depend on the initial trajectory diversity, which is limited here. The greedy scheduling assigns users sequentially to the nearest time slots without considering trajectory geometry, thereby possibly assigning consecutive time slots with poor geometry to a user. Fig. 2(b) presents the corresponding RMSE. The proposed scheme proves its outperformance compared to the baselines when implemented with a specific estimator, i.e., EKF. The RMSE trends align with the CRLB results, demonstrating the validity of minimizing CRLB.

Fig. 3(a) shows the average CRLB under different numbers

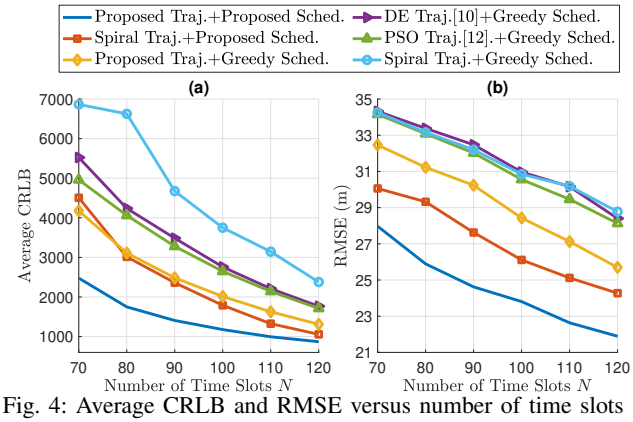

Fig. 4: Average CRLB and RMSE versus number of time slots N

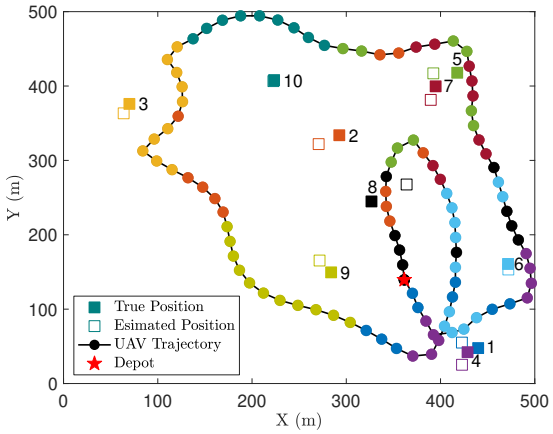

Fig. 5: A realization of UAV trajectory and users' scheduling and positions (marked with different colors) of the proposed scheme.

of users. The number of signal observations greatly impacts localization accuracy in general. As more users appear in the system, each user is assigned fewer time slots, leading to larger localization error bounds. The corresponding RMSE results in this test are shown in Fig. 3(b). We can also observe that when there are not many users in the network, e.g., $M = 4$, the difference between the schemes is less significant, as each user is assigned a sufficient number of time slots.

Fig. 4(a) examines the average CRLB with different numbers of time slots N. As more time slots are given, the UAV collects more signal observations, thereby improving the localization lower bound in all schemes. The performance of the proposed scheme is again significantly better than that of the baselines. The corresponding RMSE results in this test are presented in Fig. 4(b). According to these results, the PSO-Traj, DE-Traj, and Spiral Traj with greedy scheduling need around 120 time slots to achieve the localization error that can be obtained by the proposed scheme with fewer than 80 time slots. Therefore, the UAV in our proposed scheme is also more efficient in energy consumption than the baselines.

Fig. 5 illustrates a realization of the UAV trajectory and transmission scheduling under the proposed scheme. It can be observed that the joint optimization is designed such that the UAV collects signals from locations close to and surrounding the users. This spatial diversity improves the geometric dilution of precision (GDOP), which has a significant influence on localization accuracy [5]. Consequently, most of the estimated positions found by the EKF are near users' true positions.

V. Conclusion

Using an RSS-based localization method, this paper used a UAV as a mobile anchor to locate ground users. The formulated problem aimed to minimize the average approximate CRLB by jointly optimizing transmission scheduling and UAV trajectory. The main problem was decomposed into two subproblems, where the SCA method was adapted to solve the transmission scheduling, and a gradient descent algorithm was designed to optimize the UAV trajectory. Numerous simulation results showed that the proposed algorithm outperformed the baselines that incorporated existing algorithms in trajectory design and greedy transmission scheduling.

References

[1] H. Sallouha *et al.*, "On the ground and in the sky: A tutorial on radio localization in ground-air-space networks," *IEEE Commun. Surveys & Tuts.*, vol. 27, no. 1, pp. 218–258, 2025.

[2] C. Laoudias *et al.*, "A survey of enabling technologies for network localization, tracking, and navigation," *IEEE Commun. Surveys & Tuts.*, vol. 20, no. 4, pp. 3607–3644, 2018.

[3] M. M. Azari *et al.*, "Evolution of non-terrestrial networks from 5G to 6G: A survey," *IEEE Commun. Surveys & Tuts.*, vol. 24, no. 4, pp. 2633–2672, Aug. 2022.

[4] H. Sallouha, M. M. Azari, and S. Pollin, "Energy-constrained UAV trajectory design for ground node localization," in *Proc. IEEE Global Commun. Conf. (GLOBECOM)*, Abu Dhabi, United Arab Emirates, Dec. 2018, pp. 1–7.

[5] R. W. Ouyang, A. K.-S. Wong, and C.-T. Lea, "Received signal strength-based wireless localization via semidefinite programming: Noncooperative and cooperative schemes," *IEEE Trans. Veh. Technol.*, vol. 59, no. 3, pp. 1307–1318, 2010.

[6] O. Esrafilian, R. Gangula, and D. Gesbert, "Three-dimensional-map-based trajectory design in UAV-aided wireless localization systems," *IEEE Internet Things J.*, vol. 8, no. 12, pp. 9894–9904, June 2021.

[7] Z. Li, A. Giorgetti, and S. Kandeepan, "Multiple radio transmitter localization via UAV-based mapping," *IEEE Trans. Veh. Technol.*, vol. 70, no. 9, pp. 8811–8822, Sept. 2021.

[8] P. M. Ghari, M. Sabbaghian, and H. Yanikomeroglu, "Moving aerial anchors assisted network localization," *IEEE Trans. Wireless Commun.*, vol. 21, no. 10, pp. 7839–7851, Oct. 2022.

[9] T. Liang, T. Zhang, J. Yang, D. Feng, and Q. Zhang, "UAV-aided positioning systems for ground devices: Fundamental limits and algorithms," *IEEE Internet Things J.*, vol. 9, no. 15, pp. 13 470–13 485, Aug. 2022.

[10] Z. Wang, R. Liu, Q. Liu, J. S. Thompson, and M. Kadoch, "Energy-efficient data collection and device positioning in UAV-assisted IoT," *IEEE Internet Things J.*, vol. 7, no. 2, pp. 1122–1139, Feb. 2020.

[11] S. Bi, J. Yu, Z. Yang, X. Lin, and Y. Wu, "Joint 3-D deployment and resource allocation for UAV-assisted integrated communication and localization," *IEEE Wireless Commun. Lett.*, vol. 12, no. 10, pp. 1672–1676, Oct. 2023.

[12] M. Zhu *et al.*, "Joint data collection and sensor positioning in multi-UAV-assisted wireless sensor network," *IEEE Sensors J.*, vol. 23, no. 19, pp. 23 664–23 675, Oct. 2023.

[13] R. M. Vaghefi, M. R. Gholami, R. M. Buehrer, and E. G. Strom, "Cooperative received signal strength-based sensor localization with unknown transmit powers," *IEEE Trans. Signal Process.*, vol. 61, no. 6, pp. 1389–1403, 2013.

[14] S. Tomic, M. Beko, and R. Dinis, "RSS-based localization in wireless sensor networks using convex relaxation: Noncooperative and cooperative schemes," *IEEE Trans. Veh. Technol.*, vol. 64, no. 5, pp. 2037–2050, 2015.

[15] S. M. Kay, *Fundamentals of Statistical Signal Processing: Estimation Theory*. USA: Prentice-Hall, Inc., 1993.

[16] T. Ma and et al., "UAV-LEO integrated backbone: A ubiquitous data collection approach for B5G internet of remote things networks," *IEEE J. Sel. Areas Commun.*, vol. 39, no. 11, pp. 3491–3505, Nov. 2021.